ANALYSIS OF "SOLUTION EFFECTS" INJURY

EQUATIONS FOR CALCULATING PHASE DIAGRAM INFORMATION FOR THE TERNARY SYSTEMS NACL-DIMETHYLSULFOXIDE-WATER AND NACL-GLYCEROL-WATER

GREGORY M. FAHY, *Blood Research Laboratory, American National Red Cross, Bethesda, Maryland 20014 U.S.A.*

ABSTRACT Slowly frozen cells are said to be subject to solution effects injury. An understanding of the mechanism of solution effects injury depends upon an understanding of the compositional changes brought about in the extracellular solution during the freezing process. To facilitate analysis of the mechanisms of freezing injury during slow cooling, empirical equations have been developed which permit a description of these changes in composition for the NaCl-dimethylsulfoxide-water ternary system and for the NaCl-glycerol-water ternary system. The equations describe the region of the phase diagram in which compositional changes are brought about only as a result of the precipitation of ice. The present phase diagram equations may be rearranged to give expressions for composition variables such as water content, salt concentration, unfrozen fraction of the solution, etc., which may be employed in the analysis of the relationship between solution composition and solution effects injury.

Cells subjected to freezing can be killed in at least one of two ways. Rapidly cooled cells appear to be killed by the formation of intracellular ice (1–3). Slowly cooled cells are believed to be killed as a result of changes in extracellular solution composition accompanying extracellular freezing (4–6). The type of injury leading to damage or death during slow cooling has been termed solution effects injury (7). One major goal in theoretical cryobiology at present is to determine the relationship between cellular injury and the composition of the extracellular milieu and to use this relationship to further the elucidation of the molecular mechanisms of solution effects injury. Recent studies by Meryman et al. (8) and Mazur and coworkers (9, 10) suggest that this goal may be attainable.

The purpose of the present paper is to facilitate the study of solution effects injury by presenting equations which describe the ternary liquidus surface for the systems NaCl-dimethylsulfoxide-water and NaCl-glycerol-water. Such equations allow one to calculate the composition of a solution during freezing given its starting composition and the temperature. Alternatively, one can calculate the temperature at which a particular composition will occur given the starting composition. The ability to calculate phase diagram information directly circumvents the inconvenience and inaccuracy associated with obtaining this information by interpolation (11). The phase diagram equations can also be rearranged to yield expressions describing particular aspects of solution composition (e.g., unfrozen water content, residual unfrozen volume, salt concentration, etc.) which may be associated with biological injury. Examples of application of the phase diagram equations to the study of solution effects injury

will be presented in subsequent papers (reference 12, and Fahy, G. M., manuscript in preparation).

GENERAL APPROACH

In a dilute solution the activities of the solute and the solvent are approximately equal to their mole fractions. For this reason, the activity of the solute is approximated by unity minus the activity of the solvent. But since the activity of the solute is equal to the product of the solute mole fraction and the solute activity coefficient,

$$Xs \approx (1 - a_w)/\gamma_s, \tag{1}$$

where Xs is the solute mole fraction, a_w the activity of water, and γ_s the activity coefficient of the solute.

The simplicity of Eq. 1 and the availability of an expression for a_w as a function of temperature (13) makes Eq. 1 attractive for calculating solute mole fractions as a function of temperature during freezing. The convenience of Eq. 1 is also enhanced by the fact that the equation for a_w given by Levin et al. (13) can be shown empirically to be equivalent to the much simpler expression

$$a_w = 1 + 0.00966\ T + 4.1025 \times 10^{-5}\ T^2, \tag{2}$$

where T is the temperature in degrees Celsius.

To permit use of Eq. 1, an empirical coefficient, f, has been defined to make Eq. 3 an exact expression:

$$Xs = (1 - a_w)/f. \tag{3}$$

Eq. 3 is the defining relationship for f. (f can also be related to γ_w, the activity coefficient of water, since $Xs = 1 - Xw = 1 - a_w/\gamma_w = (1 - a_w)/f$. In addition, f may be further related to γ_s, since $\partial \ln \gamma_w / \partial \ln Xw = \partial \ln \gamma_s / \partial \ln Xs$.) From known information relating Xs and T, f values can be calculated for particular solutions. The approach here is to determine f values for many points on the liquidus surfaces of the two ternary systems of present interest and to use the results to generate general expressions for f that apply to all points of interest on the liquidus for each system. These general expressions for f can then be substituted into Eq. 3, permitting calculation of Xs for any point on the liquidus.

A knowledge of the prefreezing composition of the solution and the final value of Xs permits a complete specification of the composition of the solution at the temperature of interest. If we define

$$Xs = (n_c + 2n_n)/(n_c + 2n_n + n_w), \tag{4}$$

where Xs is the total solute mole fraction, n_c the number of moles of cryoprotectant, n_n the number of moles of NaCl, and n_w the number of moles of water, then

$$n_w = (n_c + 2n_n)(Xs^{-1} - 1). \tag{5}$$

Since the prefreezing composition is known, n_c and n_n are known. But since solution composition is changed only by conversion of water into ice (until the pseudobinary eutectic

troughs are encountered), n_c and n_n are also constant. Eq. 5 therefore permits a complete specification of the composition of the solution.

Eq. 3 permits calculation of Xs if the final temperature (and, hence, the value of a_w) is known and if f is known. It would also be useful to be able to calculate the temperature at which a particular composition of interest occurs during freezing. Combining Eqs. 2 and 3 and rearranging leads to:

$$T = -[0.7541 - (0.56865 - fXs)^{1/2}]/6.405 \times 10^{-3}, \quad (6)$$

where T is again in degrees Celsius. Knowing both Xs and f allows calculation of T from Xs.

In the calculations which follow, the molecular weights of glycerol, dimethylsulfoxide (Me_2SO), water, and NaCl are taken to be 92.09, 78.13, 18.015, and 58.44, respectively.

DETERMINATION AND APPLICATION OF f

Dimethylsulfoxide System

Fig. 1 shows several isopleths for the NaCl-Me_2SO-H_2O system. The data are taken from the work of Cocks and Brower (14) and Rasmussen and MacKenzie (15) and are supplemented (circled points) with data obtained by the author by osmometry (using an Osmette A automatic osmometer, Precision Systems, Inc., Sudbury, Mass.) Each isopleth is labeled with the value of the nonaqueous mole fraction of Me_2SO, x_M, which is defined as $x_M = n_M/(n_M + 2n_n)$, where n_M is the number of moles of Me_2SO. x_M is constant along a given isopleth and has been used in favor of R (wt. % Me_2SO/wt. % NaCl) (16) for isopleth identification to avoid graphing difficulties that arise when $R = \infty (x_M = 1.00)$.

The data given in Fig. 1 were used to derive values for both Xs and f. It may be seen from Eq. 3 that the product of f and Xs is independent of the nature of the solution and is a function

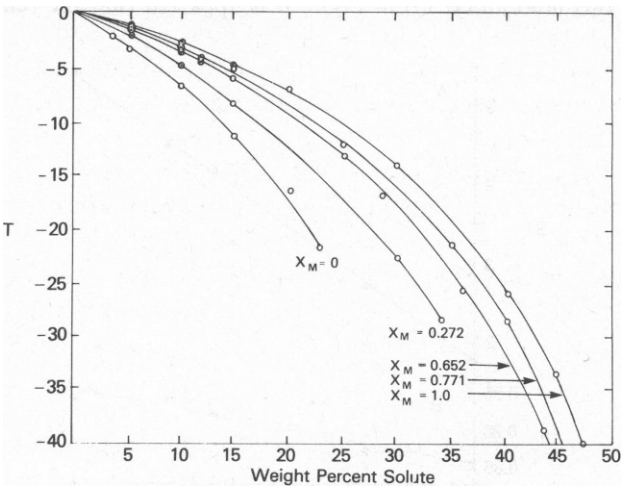

FIGURE 1 Relationship between freezing point and the total weight percentage of Me_2SO and NaCl. The curves correspond to isopleths for which the weight ratio of Me_2SO to NaCl is 0, 1, 5, 9, and ∞. The respective nonaqueous Me_2SO mole fractions for these curves (0, 0.272, 0.652, 0.771, and 1.000) are noted. The curves have been derived from the data of Cocks and Brower (14) and from osmometric determinations in this laboratory (circled points).

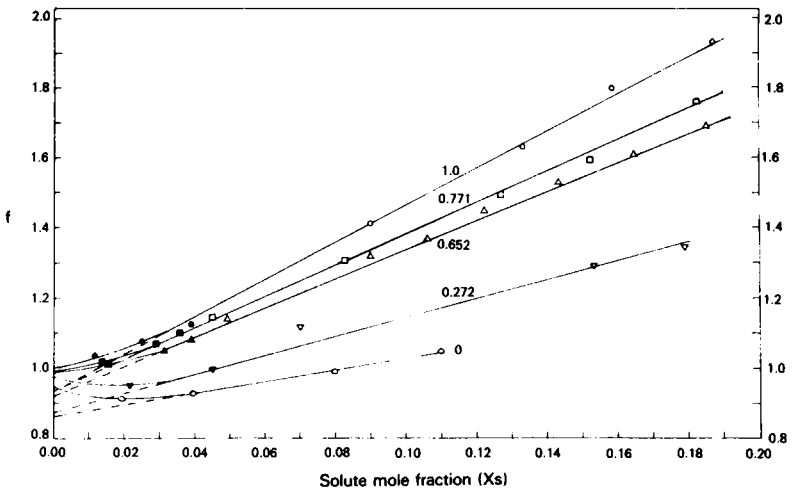

FIGURE 2 Relationship between f and Xs for different nonaqueous mole fractions of Me_2SO (noted next to each curve). Open points derived from Cocks and Brower (14); solid points derived from osmometry. $f = X^*/Xs$; see text for further details.

of temperature alone, i.e.,

$$fXs = 1 - a_w = -0.00966\ T - 4.1025 \times 10^{-5}\ T^2 = X^*. \tag{7}$$

The shorthand notation X^* has been used to emphasize that fXs depends only on temperature. Values of X^* were calculated from experimental melting points and values of f were then found by dividing X^* by the experimental Xs value determined from inspection of Fig. 1. The results are shown in Fig. 2. The solid symbols in Fig. 2 were derived from osmometric determinations in this laboratory. From Fig. 2 it is apparent that the relationship between f

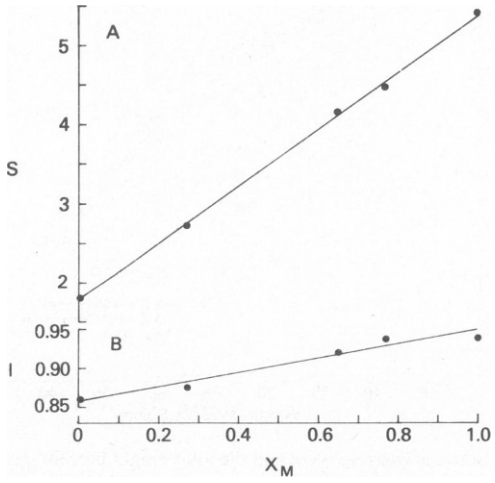

FIGURE 3 The slopes (S, Fig. 3 A) and intercepts (I, Fig. 3 B) of the linear portions of the f vs. Xs curves drawn in Fig. 2. The slopes and intercepts can both be described as linear functions of x_M, the nonaqueous mole fraction of Me_2SO. The equations of the lines drawn are given in the text (Eqs. 8 and 9).

TABLE I

EXPERIMENTAL AND CALCULATED COMPOSITIONS AND MELTING POINTS FOR THE NaCl-DIMETHYL SULFOXIDE-WATER SYSTEM

x_M	$-T_{exp}$	Xs_{exp}	Xs_{calc}	$-T_{calc}$
0.272	8.3	0.070	0.072	8.1
	22.6	0.154	0.152	23.1
	28.3	0.179	0.176	29.1
0.652	6.0	0.050	0.051	5.9
	13.0	0.090	0.092	12.6
	16.2	0.106	0.108	15.8
	25.4	0.143	0.145	24.8
	31.7	0.164	0.166	31.0
	38.8	0.185	0.187	38.2
0.771	5.5	0.045	0.046	5.4
	11.7	0.082	0.083	11.5
	21.5	0.127	0.126	21.6
	28.3	0.152	0.150	28.8
	40.0	0.186	0.183	41.1
1.000	2.7	0.025	0.024	2.8
	13.9	0.090	0.089	14.0
	25.2	0.133	0.132	25.4
	34.7	0.159	0.160	34.4
	46.9	0.187	0.187	46.8

Total solute mole fraction was calculated (Xs_{calc}) from the experimental melting point (given as the absolute value of the temperature in degrees Celsius, first column). Calculated melting points (T_{calc}, also given in negative degrees Celsius) were based on experimental solute mole fractions (Xs_{exp}). x_M is the nonaqueous mole fraction of dimethylsulfoxide, as defined in the text. Data derived from Fig. 1.

and Xs is linear along all of the isopleths studied, at least for $Xs > 0.025$. Moreover, a plot of the slopes of these lines vs. the nonaqueous mole fraction of Me_2SO is also linear, as shown in Fig. 3. Similarly, a plot of the intercepts of the lines shown in Fig. 2 against x_M is also approximately linear. The equations of the lines shown in Fig. 3 are:

$$S = 3.55\, x_M + 1.80 \tag{8}$$

and

$$I = 0.076\, x_M + 0.86, \tag{9}$$

where S is the slope (df/dXs) from Fig. 2 and I is the y intercept. Clearly,

$$f = SXs + I \tag{10}$$

for any point on the liquidus, provided Xs is > 0.025.

Substituting Eq. 10 into Eq. 3 leads to a quadratic expression for Xs with the solution:

$$Xs = [-I + (I^2 + 4SX^*)^{1/2}]/2S. \tag{11}$$

Eq. 11 is the desired relationship permitting Xs to be calculated from temperature (X^*) as a function of x_M. The temperature at which a particular solute mole fraction occurs can be calculated from

$$T = -[0.7541 - (0.56865 - SXs^2 - IXs)^{1/2}]/6.405 \times 10^{-3}. \tag{12}$$

Experimental data obtained from Fig. 1 are compared in Table I to data calculated using Eqs. 11 and 12. Mole fractions calculated from the experimental temperatures agree extremely well with the experimentally determined mole fractions. Temperatures calculated from the experimental mole fractions also compare closely with the experimental temperatures. The error of the calculations for both *Xs* and *T* is probably within the accuracy with which the original data of Cocks and Brower (14) could be read from their published figure.

Two restrictions on the use of Eqs. 11 and 12 must be stressed. The first restriction applies to solutions having a mole fraction $<\sim 0.025$. For these solutions, f values may be estimated with little difficulty by inspection of Fig. 1 and substituted directly into Eq. 3. The second restriction applies to the use of the equations below $-40°C$. Experimental data in this region

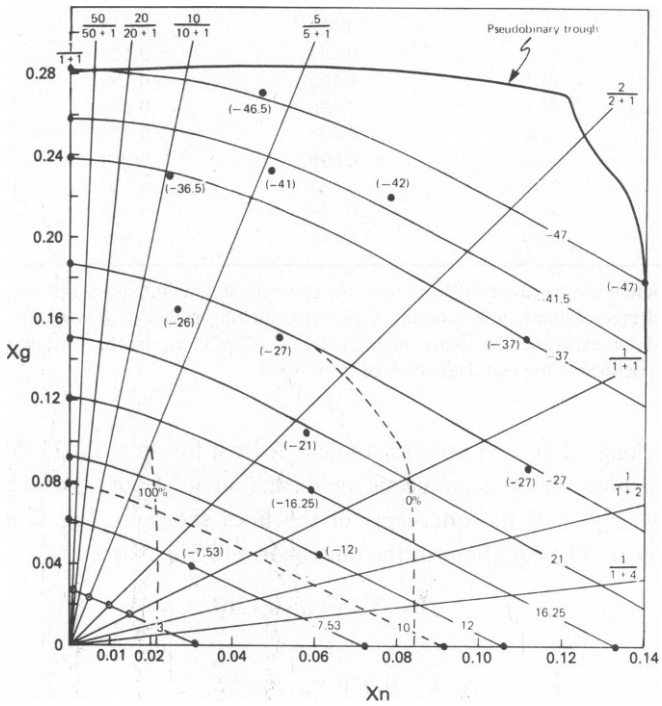

FIGURE 4 Relationship between composition and freezing point in the NaCl-glycerol-water system. Compositions are expressed in mole fraction units (*Xg* represents the mole fraction of glycerol; *Xn* represents the mole fraction of NaCl). Plotted points represent specific compositions taken from the data of Goldston (17) (closed circles) or derived from osmometry in this laboratory (circled points). Freezing points of solutions having the plotted compositions are given in parentheses next to the plotted points. Selected compositions for the glycerol-water binary system and for the NaCl-water binary system have also been plotted along the vertical and the horizontal axes, respectively, using the data of Wolf and Brown (18) and of Lane (19). The plotted binary compositions have melting points corresponding to the temperatures of the drawn isotherms; these isotherms were drawn on the basis of the temperature-composition coordinates plotted from the work of Goldston and from the binary freezing point data. Isopleths have been drawn for solutions having 50, 20, 10, 5, 2, and 1 mole of glycerol for every mole of NaCl [indicated as 50/(50 + 1), 20/(20 + 1), etc., to refer to the nonaqueous mole fraction of glycerol for each isopleth]. f values have been calculated at the intersections between the isotherms and the isopleths and are plotted in Fig. 5. The two approximately vertical dashed lines in Fig. 4 refer to the region within which survival of human red cells ranges from ~100% to 0% (20).

are limited. In addition, there is some indication of a discontinuity in the shape of the composition-temperature curve at ~ −40°C (14). Further research will be necessary to extend mathematical models of the liquidus to temperatures below −40°C.

Glycerol System

Data for the NaCl-glycerol-water system were obtained from the work of Goldston (17). Unlike the data of Cocks and Brower (14), Goldston's data do not describe particular isoplethal sections. In view of the utility of isoplethal freezing point data, such data have been derived from the data of Goldston as indicated in Fig. 4.

Fig. 4 is a plot of the mole fraction of glycerol (Xg) vs. the mole fraction of NaCl (Xn) in the ternary system. The two axes are drawn on different scales after Shepard et al. (16) to show sufficient detail. Selected data points of Goldston are plotted and the melting point for each plotted composition is noted next to the plotted point. Isotherms joining the plotted points and the appropriate binary mole fractions along the two axes have been drawn. The extraction of the desired information is completed by drawing appropriate isopleths (represented by the straight lines emanating from the origin) and noting the temperature-composition coordinates given by the intersections between the isopleths and the isotherms. X^* values were calculated from the temperatures and divided by the Xs values at the insections to obtain f values for the intersection points. The results are displayed in Fig. 5.

Several interesting features of the NaCl-glycerol-water system are apparent in Fig. 5. f values tend to be relatively low and relatively insensitive to solution composition, a factor which places limits on the absolute errors associated with determination of f values. The dependence of f on Xs is linear as was the case for the Me_2SO system, but in the glycerol system two straight lines are required to describe a given isopleth. This bending of the f vs. Xs curve is characteristic of glycerol rather than of NaCl. The behavior of the system is similar to the behavior of glycerol provided that the nonaqueous mole fraction of glycerol (x_g) is

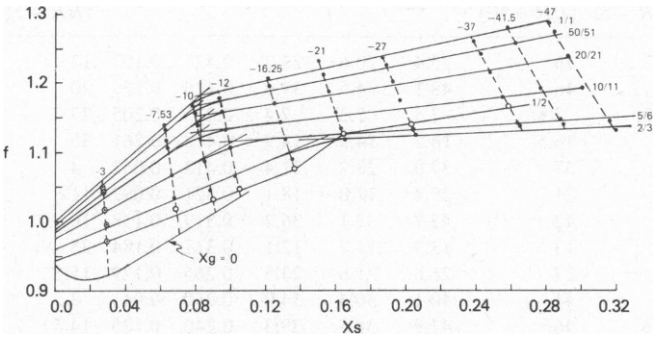

FIGURE 5 Relationship between f and Xs for different nonaqueous mole fractions of glycerol (indicated next to each line). Open points refer to $x_g = 0.50$; circled points refer to data from osmometry. All points have been derived from the intersections between the isopleths and the isotherms in Fig. 4, as indicated. The curves are linear at both high and low Xs values, but show a break (indicated by vertical and horizontal lines) at intermediate values. The region to the left of and below these break points will be referred to as the dilute region; the remaining area will be referred to as the concentrated region of the figure. Different equations apply to these two different temperature-composition regimes. The straight lines for the two regions have been extended in the vicinity of the break points to indicate the proximity of the extended lines to the smooth curve in the area of the break points.

two-thirds or above. Between $x_g = 0.667$ and $x_g = 0.5$ the influence of NaCl becomes apparent, particularly at higher Xs values, where the slope of the f vs. Xs curve begins to approach the slope of the corresponding curve for the NaCl-water binary system. In fact, for $x_g = 0.5$, the break in the f vs. Xs curve can be considered to be absent since extrapolation of the curve in the dilute region to temperatures as low as -37°C is possible with errors in f no greater than 2%. The break in the f vs. Xs curve is even less apparent for $x_g < 0.5$ (data not shown).

The equations which follow have been derived for solutions having $x_g \geq 0.5$. It will be shown, however (Table II), that these equations can be extrapolated to $x_g = \sim 0.15$ with good accuracy. A solution of $x_g = 0.5$ in which cells are to be suspended before freezing would have a glycerol concentration of ~ 0.32 M, or $\sim 2.3\%$ by volume.

Fig. 6 A shows the dependence of the slope, df/dXs, or S, on x_g for the dilute region of Fig. 5. The experimental points are fitted well by:

$$S = 7|x_g - 0.5|^{2.5} + 0.955, \tag{13}$$

which is also sketched in Fig. 6 A. Fig. 6 B displays the relationship between the y intercepts of the f vs. Xs lines and x_g for the dilute region; the points can be described by:

$$I = 0.099\, x_g + 0.895. \tag{14}$$

The slopes for the more concentrated region of Fig. 5 are shown in Fig. 7 A. As is apparent in

TABLE II
EXPERIMENTAL COMPOSITIONS AND CALCULATED MELTING POINTS FOR THE NaCl-GLYCEROL-WATER SYSTEM

$x_g \geq 0.5$							$x_g < 0.5$				
x_g	Xs	$-Te$ ($HR = 5$)	$-Te$ ($HR = 10$)	$-T_{calc}$	$-T_I$	$-T_{IC}$	x_g	Xs	$-Te$ ($HR = 5$)	$-Te$ ($HR = 10$)	$-T_{calc}$
0.556	0.194	25	26	25.4	20.6	22.2	0.427	0.107	12	12	12.2
0.559	0.318	47	46	48.1	34.5	39.6	0.426	0.159	20	20	19.6
0.561	0.069	7.25	7.8	7.5	7.2	7.4	0.425	0.205	27	27	27.1
0.562	0.135	16	16.5	16.2	14.2	14.9	0.418	0.261	35	37.5	38.4*
0.569	0.263	37	37	37.0	28.2	31.4	0.413	0.052	4	5	5.4
0.644	0.161	21	21	20.4	17.0	18.1	0.321	0.092	11	11	10.2
0.738	0.297	42	42	42.1	32.1	36.2	0.319	0.138	16	17	16.5
0.738	0.111	14	13	13.3	11.7	12.1	0.317	0.184	25	24	23.7
0.749	0.204	27	27	26.6	21.6	23.5	0.265	0.129	15.5	15	15.3
0.826	0.282	41	41	40.1	30.4	34.0	0.250	0.041	3.5	4	4.2
0.853	0.318	47.5	46	47.9	34.5	39.3	0.240	0.125	14.5	14.5	14.7
0.864	0.190	25	27	25.1	20.2	21.7	0.238	0.168	21.5	23	21.4
0.905	0.255	37	36	36.9	27.3	30.2	0.173	0.116	13.5	13.5	13.7

x_g is the nonaqueous mole fraction of glycerol. Xs is the total solute mole fraction. Te represents the experimental melting point determined by differential thermal analysis at a heating rate of either 5 or 10°C/min ($HR = 5$, $HR = 10$). T_{calc} was calculated from Eq. 12. T_I (for ideal solutions) was calculated from Eq. 17. T_{IC} (for ideal solutions, corrected for changes in the latent heat of fusion with temperature) was calculated using Eq. 19. Experimental data of Goldston (17).

*$T_{calc} = -37.5$ if Eqs. 15 and 16 are used for S and I. Eqs. 13 and 14 have been used for all solutions having $x_g < 0.5$.

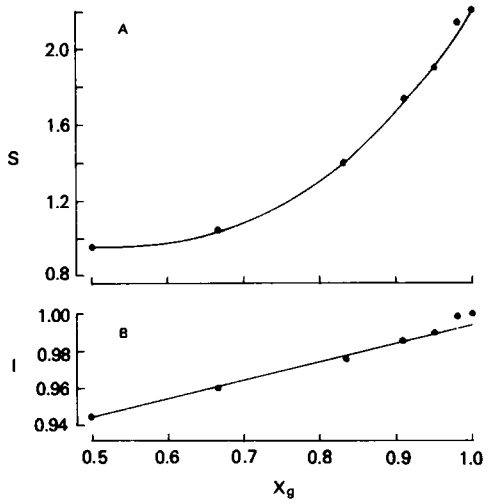

FIGURE 6 (*A*) Slopes (*S*) of the straight lines in the dilute region of Fig. 5 as a function of the nonaqueous mole fraction of glycerol (x_g). The equation of the curve drawn is given in the text (Eq. 13). (*B*) Intercepts (*I*) of the lines in the dilute region of Fig. 5 as a function of x_g. The line drawn joining the points is given by Eq. 14.

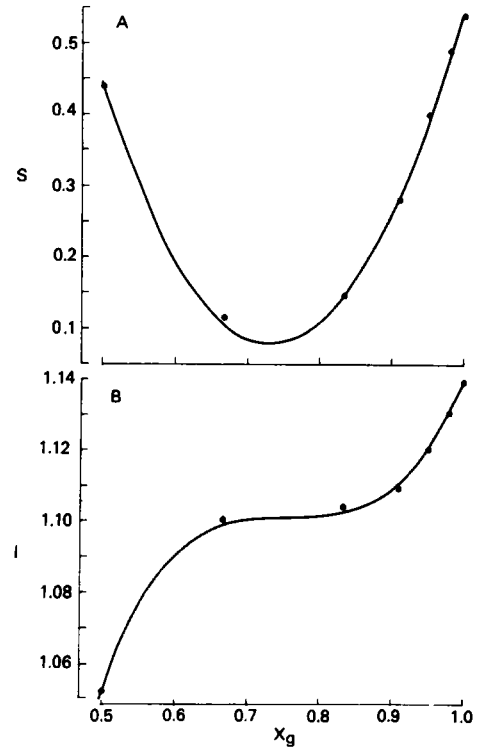

FIGURE 7 (*A*) Slopes (*S*) of the *f* vs. *Xs* curves in the concentrated region of Fig. 5 as a function of x_g. The curve drawn connecting the plotted points is given by Eq. 15. (*B*) *y*-intercepts (*I*) of the lines in the concentrated region of Fig. 5. The dependence of *I* on x_g is described by Eq. 16.

the figure, the slopes are fitted well by the parabolic relationship:

$$S = 6.536(x_g - 0.732)^2 + 0.080. \tag{15}$$

The intercepts (Fig. 7 *B*) may be calculated quite accurately from:

$$I = 2.8(x_g - 0.77)^3 + 1.101. \tag{16}$$

Eqs. 11 and 12 may now be solved for the NaCl-glycerol-water system using Eqs. 13–16 to supply the appropriate values for S and I. The conditions under which Eqs. 13 and 14 should

SCHEME I
GUIDE FOR USING TERNARY PHASE DIAGRAM EQUATIONS

(*A*) Definitions and Conventions.

1. n_c, n_n, and n_w refer to the number of moles of cryoprotectant (glycerol or Me_2SO), NaCl, and liquid water, respectively. n_c and n_n are considered constant, with composition changing as a result of changes in n_w.

2. $Xs = (n_c + 2n_n)/(n_c + 2n_n + n_w)$, where Xs is the total solute mole fraction; using this relationship, knowledge of n_c and n_n, and a calculated value of Xs, it is possible to calculate the value of n_w.

3. $x_M = n_M/(n_M + 2n_n)$ and $x_g = n_g/(n_g + 2n_n)$, where x_M and x_g are the nonaqueous mole fractions of Me_2SO and of glycerol, respectively, and n_M and n_g refer to the number of moles of Me_2SO and of glycerol.

4. The molecular weights of Me_2SO, glycerol, water, and NaCl are taken to be 78.13, 92.09, 18.015, and 58.44, respectively.

(*B*) Calculation of mole fraction of solute as a function of temperature:

$$Xs = [-I + (I^2 - 0.03864\,ST - 1.641 \times 10^{-4}\,ST^2)^{1/2}]/2S,$$

where T is the temperature in degrees Celsius.

(*C*) Calculation of temperature at which a particular composition occurs:

$$T = -[0.7541 - (0.56865 - SXs^2 - IXs)^{1/2}]/6.405 \times 10^{-3},$$

where again T is given in degrees Celsius.

(*D*) Calculation of S and I: NaCl-Me_2SO-H_2O system:

$$S = 3.55\,x_M + 1.8 \text{ and } I = 0.076\,x_M + 0.86.$$

Note: Use only if $Xs \geq 0.025$ and if T is above $-40°$ to $-50°$C.

(*E*) Calculation of S and I: NaCl-glycerol-H_2O system:
Dilute region (equations D1 and D2):

$$S = 7|x_g - 0.5|^{2.5} + 0.955 \qquad I = 0.099\,x_g + 0.895$$

Concentrated region (equations C1 and C2):

$$S = 6.536\,(x_g - 0.732)^2 + 0.08 \text{ and } I = 2.8\,(x_g - 0.77)^3 + 1.101.$$

Note: Use equations D1 and D2 for $x_g < 0.5$. If $0.5 < x_g \leq 0.87$, use D1 and D2 if $f < 1.12$ and C1 and C2 if $f > 1.12$; if $x_g \geq 0.87$, use D1 and D2 for $Xs \leq 0.083$ and C1 and C2 for $Xs \geq 0.083$. Do not use D1 and D2 if T is above $\sim -4°$C and $x_g < 0.5$.

(*F*) For regions in which f cannot be calculated from S and I ($f = SXs + I$), f may be determined by direct inspection of Figs. 2 or 5 if Xs is known; if Xs is not known, Xs and f may be determined by iterative solution of the following equation using Figs. 2 or 5 as a guide: $Xs = (-0.00966\,T - 4.1025 \times 10^{-5}\,T^2)/f$, where T is in degrees Celsius.

be used rather than Eqs. 15 and 16 are delineated in Scheme I, in which the phase diagram equations and their restrictions are summarized.

Table II presents a comparison between the experimental data of Goldston (18) and the predictions of Eq. 12 as solved for the glycerol system. The agreement between the experimental and the calculated freezing points is quite good, even for x_g as low as 0.173. Also shown for comparison are freezing points calculated using the usual thermodynamic approximation:

$$T = [R\Delta H_f^{\circ -1}\ln(1-Xs) + 273.15^{-1}]^{-1} - 273.15. \quad (17)$$

(T = °C; ΔH_f°, the latent heat of fusion at 0°C, is −1,436 cal/mol; R, the universal gas constant, is 1.987 cal/°−mol), which is equivalent to the expression used by Mazur (21) in modeling the kinetics of water efflux from cells during freezing. Eq. 17 assumes that ΔH_f° is independent of temperature (22–24). If this assumption is removed, using

$$\Delta H_f = \Delta H_f^\circ + \Delta c_p(T - 273.15), \quad (18)$$

where Δc_p is the difference between the heat capacities of ice and water and is considered

TABLE III
COMPARISON BETWEEN CALCULATED COMPOSITION/MELTING POINT DATA AND DATA OBTAINED FROM SHEPARD ET AL.,* WOLF AND BROWN,‡ AND LANE§

x_g	Xs_{exp}	Xs_{calc}	T_{exp}	T_{calc}
0.241*	0.089	0.090	−10	−9.9
	0.166	0.159	−20	−21.1
	0.223	0.215	−30	−31.6
0.388*	0.094	0.090	−10	−10.4
	0.158	0.162	−20	−19.4
	0.225	0.220	−30	−31.0
0.559*	0.090	0.089	−10	−10.1
	0.154	0.158	−20	−19.4
	0.216	0.223	−30	−28.9
	0.285	0.279	−40	−41.3
0.741*	0.082	0.087	−10	−9.4
	0.153	0.159	−20	−19.2
	0.223	0.226	−30	−29.5
	0.284	0.285	−40	−39.8
1.000	0.021‡	0.021	−2.3	−2.3
	0.047‡	0.047	−5.5	−5.5
	0.077‡	0.076	−9.5	−9.7
	0.115‡	0.116	−15.4	−15.3
	0.164§	0.164	−23.0	−23.1
	0.193§	0.193	−28.2	−28.2
	0.227§	0.227	−34.7	−34.7
	0.267§	0.272	−44.6	−43.4

x_g, nonaqueous mole fraction of glycerol; Xs_{exp}, solute mole fraction obtained from cited references; Xs_{calc}, solute mole fraction calculated (Eq. 11) using T_{exp}, the melting point obtained from cited reference; T_{calc}, temperature calculated from Xs_{exp} using Eq. 12.
*Reference 16.
‡Reference 18.
§Reference 19.

constant at -9.7 cal/°−mol (21), Eq. 17 becomes

$$610.75(T^\circ - T)/TT^\circ + 4.882 \ln(T/T^\circ) = \ln(1 - Xs), \quad (19)$$

where $T^\circ = 273.15$°K and T is given in degrees Kelvin. Temperatures calculated from Eq. 19 are also given in Table II. It is clear that Eq. 12 represents a substantial improvement over both Eq. 17 and Eq. 19. It should be pointed out that the predictions of Eq. 19 are almost identical to the predictions of Eq. 6 for an ideal solute ($f = 1.0$).

SCHEME II

CALCULATION OF PHASE DIAGRAM INFORMATION USING CONCENTRATION UNITS OTHER THAN MOLE FRACTION

(*A*) Calculation of Solute Concentrations as a Function of Temperature

1. First calculate the nonaqueous mole fraction of cryoprotective agent (cpa) as follows:

$x_c = Mc/(Mc + 2Mn)$ (Mc = molarity of cpa; Mn = molarity of NaCl)

$x_c = m_c/(m_c + 2m_n)$ (m_c = molality of cpa; m_n = molality of NaCl)

$x_c = (Wc/MWc)/(Wc/MWc + 2Wn/MWn)$ (Wc = weight percentage of cpa; Wn = weight percentage of NaCl; MWc = cpa mol wt; MWn = mol wt of NaCl)

$x_c = (Vc/\overline{V}c)/[Vc/\overline{V}c + 2w_n/MWn)$ (Vc = percentage of cpa by volume; w_n = the percentage of NaCl expressed as wt/vol; $\overline{V}c$ = the volume of 1 mol cpa; for glycerol, $\overline{V}c$ is taken to be 73.09 ml/mol; for Me_2SO, $\overline{V}c$ is taken to be 71.03 ml/mol)

2. Calculate S and I as described in Scheme I.
3. Calculate Xs from T using the equation given in Scheme I, section *B*.
4. Calculate CF, the factor by which the concentration (in convenient units) has been elevated during freezing.

The molar concentration factor:

$CF_M = 1{,}000/[Vs + 18.015\ (Mc_o + 2Mn_o)\ (Xs^{-1} - 1)]$, where Vs is the volume of the solute (cpa plus NaCl), Mc_o and Mn_o are the initial molarities of cpa and NaCl, respectively, and Xs is the total solute mole fraction as calculated from the equation given in Scheme I, section *B*. $Vs = Mc_o\overline{V}c + 26.99\ Mn_o$.

The molal concentration factor:

$CF_m = 55.51/(m_{c_o} + 2m_{n_o})\ (Xs^{-1} - 1)$, where m_{c_o} and m_{n_o} are the initial molalities of cpa and NaCl, respectively.

The volumetric concentration factor:

$CF_V = 100/[Vs + 18.015\ (Vc_o/\overline{V}c + 2w_{n_o}/MWn)(Xs^{-1} - 1)]$, where Vs, the volume of solute, equals $Vc_o + 26.99\ w_{n_o}/MWn$ and Vc_o and w_{n_o} are the initial percent by volume of cpa and percent wt/vol of NaCl, respectively.

CF_V is numerically identical to CF_M.

The weight percent concentration factor:

$CF_W = 100/[Wc_o + Wn_o + 18.015\ (Wc_o/MWc + 2Wn_o/MWn)(Xs^{-1} - 1)]$, where Wc_o and Wn_o are the initial weight percentages of cpa and NaCl, respectively.

5. To find the final concentration of salt and cpa, multiply the initial concentration by the appropriate concentration factor.

(*B*) Calculation of Temperatures Corresponding to Particular Solute Concentrations

1. First calculate the Xs value corresponding to the particular CF of interest.

$Xs = [(1{,}000/CF_M - Vs)/18.015(Mc_o + 2Mn_o) + 1]^{-1}$

$Xs = [55.51/(m_{c_o} + 2m_{n_o})CF_m + 1]^{-1}$

$Xs = [(100/CF_V - Vs)/18.015\ (Vc_o/\overline{V}c + 2w_{n_o}/MWn) + 1]^{-1}$

$Xs = [(100/CF_W - Wc_o - Wn_o)/18.015\ (Wc_o/MWc + 2Wn_o/MWn) + 1]^{-1}$

2. Second, calculate x_c, S, and I as described above.
3. Finally, calculate the temperature from the equation given in Scheme I, section *C*.

Table III gives a comparison between freezing points obtained from the curves given by Shepard et al. (16) and freezing points calculated using Eq. 12. The agreement between the two sets of data supports the reliability of both the computer smoothed curves of these authors and Eq. 12. Table III also provides a comparison between experimental and calculated freezing points for the glycerol-water binary system, indicating the excellent agreement between the data and the calculations.

CONCLUSION

Ternary phase diagram equations have been developed for the NaCl-Me_2SO-H_20 system and for the NaCl-glycerol-H_20 system which permit accurate calculation of compositional data given initial composition and final temperature and which permit calculation of the temperature at which a particular composition of interest will occur during freezing, given the starting composition (see Schemes I and II for a summary of the equations and the restrictions on their use). The area of the liquidus surface described by the ternary phase diagram equations is the water-rich region bounded by the pseudobinary eutectic troughs, and calculations consequently should not be extended beyond the lines of twofold saturation, where supersaturation, solute precipitation, and glass formation are all possible. The equations apply accurately only when cooling is slow enough to permit equilibrium conditions to be approached, and only when the final temperature is $>\sim -50°C$. Despite these restrictions, the present equations do provide a useful means of relating survival data and composition data in the temperature range of greatest interest, where most solution effects injury will occur.

A portion of this research was completed in partial fullfillment of the requirements for the Doctor of Philosophy degree in pharmacology at the Medical College of Georgia.

This research was supported in part by grants M 17816-02 and GM 17959 from the U. S. Public Health Service, National Institutes of Health. This paper is Contribution No. 443 from the American National Red Cross.

Received for publication 29 December 1979 and in revised form 19 June 1980.

REFERENCES

1. MAZUR, P. 1977. The role of intracellular freezing in the death of cells cooled at supraoptimal rates. *Cryobiology.* **14**:251–272.
2. BANK, H. 1973. Visualization of freezing damage. II. Structural alterations during warming. *Cryobiology.* **10**:157–170.
3. MERYMAN, H. T. 1956. The mechanics of freezing in living cells and tissues. *Science (Wash., D. C.).* **124**:515–521.
4. PEGG, D. E. 1976. Long-term preservation of cells and tissues: a review. *J. Clin. Pathol. 29:271–285.*
5. MAZUR, P. 1977. Slow-freezing injury in mammalian cells.*In* The Freezing of Mammalian Embryos. K. Elliot and J. Whelan, editors. Elsevier/Excerpta Medica, New York. 19–42.
6. MERYMAN, H. T. 1974. Freezing injury and its prevention in living cells. *Ann. Rev. Biophys. Bioeng.* 3:341–363.
7. MAZUR, P. 1970. Cryobiology: the freezing of biological systems. *Science (Wash., D. C.).* **168**:939–949.
8. MERYMAN, H. T., R. J. WILLIAMS, and M. St. J. DOUGLAS. 1977. Freezing injury from solution effects and its prevention by natural or artificial cryoprotection. *Cryobiology.* **14**:287–302.
9. MAZUR, P., and W. F. RALL. 1979. Role of solute composition and concentration vs. channel size on slow-freezing injury in human red cells. I. phase relations. *Cryobiology.* **16**:587.
10. MAZUR, P., N. RIGOPOULOS, and R. WEISS. 1979. Role of solute composition and concentration vs. channel size on slow freezing injury in human red cells. II. Survival vs. phase relations. *Cryobiology.* **16**:587.
11. RALL, W.F., P. MAZUR, and H. SOUZU. 1978. Physical-chemical basis of the protection of slowly frozen human red cells by glycerol. *Biophys. J.* **23**:101–120.

12. FAHY, G. M. 1980. Analysis of "solution effects" injury: rabbit renal cortex frozen in the presence of dimethylsulfoxide. *Cryobiology.* **17**:371–388.
13. LEVIN, R. L., E. G. CRAVALHO, and C. E. HUGGINS. 1976. Effect of hydration on the water content of human erythrocytes. *Biophys. J.* **16**:1411–1426.
14. COCKS, F. H., and W. E. BROWER. 1974. Phase diagram relationships in cryobiology. *Cryobiology.* **11**:340–358.
15. RASMUSSEN, D. H., and A. P. MACKENZIE. 1968. Phase diagram for the system water-dimethylsulfoxide. *Nature (Lond.).* **220**:1315–1317.
16. SHEPARD, M. L., C. S. GOLDSTON, and F. H. COCKS. 1976. The H_20-NaCl-glycerol phase diagram and its application in cryobiology. *Cryobiology.* **13**:9–23.
17. GOLDSTON, C. S. 1974. Determination of the H_20 rich region of the H_20-NaCl-glycerol system by differential analysis techniques. M.S. Thesis, Duke University, Durham, N.C.
18. WOLF, A. V., and M. G. BROWN. 1968. Concentrative properties of aqueous solutions: conversion tables. *In* Handbook of Chemistry and Physics, 49th Edition, R. C. Weast, editor. The Chemical Rubber Company, Cleveland, Ohio. D143-D182.
19. LANE, L. B. 1925. Freezing points of glycerol and its aqueous solutions. *Ind. Engr. Chem.* **17**:924.
20. LOVELOCK, J. E. 1953. The mechanism of the protective action of glycerol against haemolysis by freezing and thawing. *Biochim. Biophys. Acta.* **11**:28–36.
21. MAZUR, P. 1963. Kinetics of water loss from cells at subzero temperatures and the likelihood of intracellular freezing. *J. Gen. Physiol.* **47**:347–369.
22. LEWIS, G. N., and M. RANDALL. 1961. Thermodynamics, Second Edition, revised by Kenneth S. Pitzer and Leo Brewer. McGraw-Hill, New York.
23. KLOTZ, I. M. 1953. Chemical Thermodynamics, Basic Theory and Methods. Prentice Hall, New York.
24. DANIELS, F., and R. A. ALBERTY. 1966. Physical Chemistry, Third Edition. John Wiley & Sons, Inc., New York.